J. COMBIN. MATH. COMBIN. COMPUT. 127a (2025) 6181--6197

Journal of Combinatorial Mathematics and Combinatorial Computing
www.combinatorialpress.com/jcmcc

Combinatorial Press

Deep Learning-based Recognition and Quantification of Cultural Identity Features in Chinese Oil Painting Art

Yan Gao[1,✉]

[1] *Jiangsu Vocational College of Electronics and Information, Huaian, Jiangsu, 223301, China*

ABSTRACT
Chinese oil painting art is an important carrier of contemporary Chinese cultural identity features, the identification and quantitative study of the color and texture of the picture can help to understand the characteristics of the oil painting works more deeply. Therefore, this paper proposes a feature recognition method for oil painting art based on deep learning method. The Otsu threshold method and DeeplabV3+ network model based on DeeplabV3+ are selected for image graying and segmentation processing. The global color histogram and ring LBP are used to extract the color and texture features of the picture respectively, and the oil painting feature recognition is completed based on the regularized limit learning machine. In several sets of quantitative results, the methods in this paper all have better oil painting color and texture feature recognition, among which the RELM algorithm has the highest detection accuracy at low correlation features. It shows that the deep learning based Chinese oil painting art and cultural identity feature recognition method can effectively extract oil painting features and realize the quantitative research on oil painting.

Keywords: LBP, global color histogram, deep learning, otsu thresholding method, oil painting identity recognition

1. Introduction

Deep learning algorithm is a kind of machine learning technology that simulates the learning and processing ability of human brain neural network through multi-level neural network structure. Its core idea is to realize the abstraction and characterization of input data by constantly adjusting the connection strength between neurons, so as to achieve automatic learning and solving of complex problems. It is of great significance in natural language processing, image recognition and classification art, especially in the identification and quantification of cultural identity features of Chinese oil painting art [1-4].

✉ Corresponding author.
E-mail address: gaoyanhuashi2004@163.com (Y. Gao).
Received 05 March 2024; Revised 25 May 2024; Accepted 05 December 2024; Published Online 15 April 2025.
DOI: 10.61091/jcmcc127a-340

As one of the important genres in the history of Chinese art, Chinese oil painting, since its introduction to China at the beginning of the 20th century, can be divided into three stages of development. The first stage is the imitation stage. This stage is mainly to refer to western paintings, and to imitate and learn from them. The imitation stage is mainly from the beginning of the 20th century to 1959, most of the works in this stage adopt the realism method and skillful expression techniques, but the subject matter is simple and the creativity is relatively single [5-8]. The second stage is the exploration stage. In this stage, mainly from 1960 to 1990, artists began to seek their own creative ideas and styles. Artists began to diversify their creative methods, influenced by traditional Chinese culture. The oil paintings in this period were characterized by national style and modernism, and were noticed and recognized by the outside world [9-12]. The third stage is the diversified stage. This stage is mainly the modern stage from 1990 to the present. Chinese oil paintings in this period show diversified characteristics, not only realism, but also abstraction and expressionism, as well as liberal creative styles. In addition, in this era, more and more Chinese oil painters have won international awards, including many world-class masters [13-16]. With the deepening of reform and opening up and the continuous development of China's economy, Chinese oil painting has made brilliant achievements in art creation, market demand and art education [17-18].

In this paper, oil painting images are preprocessed such as graying and segmentation using Otsu thresholding method and DeeplabV3+ based network model. The global color histogram is used to extract the color features of Chinese oil paintings, and the images in RGB format are converted to HSV space. In view of the robustness of illumination, the article adopts the selection of improved cyclic LBP algorithm and grayscale covariance matrix to extract the local texture features of oil paintings. In order to improve the accuracy of Extreme Learning Machine Model (ELM) and introduce regularization factor to avoid overfitting, the RELM model is designed and used for oil painting color and texture feature recognition. A collection of Chinese oil paintings is taken as a sample, and the method of this paper is used to quantitatively analyze the spectral features, texture features and artistic and cultural identities of the oil painting subjects to test the practicality of the method of this paper.

2. Oil painting image pre-processing

Oil painting image preprocessing is a very important preliminary work, because the data set obtained from oil painting image acquisition often has many bad influencing factors, so it will be preprocessed before feature extraction. Generally in recognition methods based on traditional feature extraction, in order to facilitate the extraction of object features, the image will be segmented, cropped and other operations. In recognition methods based on deep learning, due to the small size of most domain-specific datasets, operations such as cropping, flipping, etc. are usually used to enhance the dataset in order to obtain better experimental results.

2.1. Graying

Usually, cameras capture color images in RGB format, and when extracting some features, it is necessary to calculate all the pixel points, which is obviously very time-consuming and arithmetic power. Image grayscaling converts a three-channel image into a single-channel image, which reduces the amount of computation for subsequent operations by about two-thirds. In this paper, we need to extract the texture and edge gradient features of the object image, so we need to grayscale the image. In this paper, we use the most classic weighted average method, which assigns different weights to the R, G and B channels, and weights the three channels according to the weights to obtain a single channel value, as shown in Equation (1):

$$f(i,j)=0.30R(i,j)+0.59G(i,j)+0.11B(i,j) \tag{1}$$

Where, i, j denote the positional information of the pixel value in the image, respectively, and $f(i,j)$ is the gray value obtained.

2.2. Image Segmentation

Image segmentation extracts regions of interest in an image mainly through certain operations and has a key role in many tasks of image processing. The purpose of image segmentation in this paper is to separate the oil painting object from the background to prevent the interference of the background during subsequent feature extraction. Therefore, in this paper, Otsu thresholding method and DeeplabV3+ network model based segmentation method are used to segment the oil painting object dataset respectively.

Since the public dataset used in this paper is simple and easy to segment, and the Otsu thresholding method can get better segmentation results simply and quickly for this case [19], this paper uses the Otsu interpolation method to perform segmentation operations on the public dataset. Assuming that the size of the object image to be segmented is $M \times N$, after inputting the grayscale map after grayscaling as mentioned above, the computational process of segmenting the image by Otsu thresholding method is as follows. Assuming that the grayscale is divided into L levels, μ_i represents the ratio of the number of pixels of level i to the number of pixels in the whole image, as shown in equation (2):

$$\mu_i = \frac{N_i}{MN} \tag{2}$$

Then, according to the Otsu threshold method, the optimal inter-value T can be calculated by equation (3):

$$T = \underset{0 \le t \le L-1}{\arg\max}\left[\mu_a\left(w_a - w_0\right)^2 + \mu_b\left(w_b - w_0\right)^2\right] \tag{3}$$

Where, μ_a, μ_b are the ratio of the number of pixels in the foreground object portion and the background portion to the total number of pixels in the image, respectively. w_a, w_b are the average gray values of the foreground and background, respectively. w_0 denotes the total average gray value of the image. The above parameters are calculated according to equations (4) to (8) respectively:

$$\mu_a = \sum_{i=1}^{T} \mu_i \tag{4}$$

$$\mu_b = \sum_{i=T+1}^{L} \mu_i \tag{5}$$

$$w_a = \sum_{i=1}^{T} i\frac{\mu_i}{\mu_a} \tag{6}$$

$$w_b = \sum_{i=T+1}^{L} i\frac{\mu_i}{\mu_b} \tag{7}$$

$$w_0 = \sum_{i=1}^{L} i\mu_i \tag{8}$$

The entire gray level is traversed and finally the image is segmented based on the value with the highest inter-class variance.

3. Chinese oil painting feature extraction method

3.1. Global color histogram

Color is the most basic feature of an image to express emotion, and has been used by artists to induce emotion in images. Many studies have been done to change the emotion of an image by changing its color or combination of colors to give different emotional stimuli to the observer. Whether observed from an artistic or psychological point of view, the color or combination of colors in an image can bring strong emotional stimulation to the observer. Color to a certain extent affects the emotional expression of the image, when different hues of the image is shown to the observer, from the intuitive visual stimulation of the emotional experience is different: when the display of the image of the color tone bright, bright brightness, the emotional category is generally positive (pleasure, excitement, satisfaction or awe). When the color tones are dark and the luminance is gloomy, the emotion tends to be negative (disgust, anger, fear, or sadness).

Common global color feature extraction methods mainly include: color histogram, color moments and color entropy, and later researchers and scholars have also proposed some improved methods, such as improved color histograms, color aggregation vectors, color correlation diagrams and so on. Global color histogram describes the proportion of different colors in the whole image, which is simple and convenient, with translation, scale and rotation invariance, so in this paper, the global color histogram is chosen to extract the color features of the image [20].

The hue, saturation and luminance (HSV) of an image will directly affect the emotion of the image. In view of this, this paper selects the HSV color space, first of all, the RGB format image is converted to the HSV space, using the hue-saturation two-dimensional histogram (H-S) method, the $H-S$ space is divided into 16 hues, each hue is divided into 8 saturations, then each image can be represented as a total of 128-dimensional vectors, and then the probability of the largest dimension is converted to a 128-dimensional one-hot coding. Let the color of an image is composed of N levels, each color value is represented by q_i, $i=1,2,\ldots,N$. Then in the whole image, the dominant color is shown by equations (9), (10):

$$H\left(q_i\right)=\frac{num\left(q_i\right)}{num\left(total\right)}\left(i=1,2,\ldots,N\right) \tag{9}$$

$$C=\arg\max_{q_i} H\left(q_i\right) \tag{10}$$

Where, $num\left(q_i\right)$ denotes the number of pixel values for color qi and $num\left(total\right)$ denotes the total number of pixels in the image. $H\left(q_i\right)$ denotes the frequency of occurrence of color at each level. And this set of color statistics $H\left(q_1\right)\ldots H\left(q_N\right)$ forms the color histogram of the image. The maximum value C of this set of color statistics is taken as the dominant color of the whole image and then C is converted into 128 dimensional one-hot vector. Thus this vector in HSV space is used as the color feature of the image and is denoted as x_1.

3.2. LBP texture features

In the identification of oil painting images, in addition to color features, oil painting texture features are another important feature. The influence of texture features on emotion may not be as intuitive and strong as color, but with the spatial frequency factor contained in texture, different textures can produce different visual effects. Smoothness gives a sense of delicacy, softness gives warmth, roughness gives a sense of old age, and hardness gives a sense of rigidity. Commonly used features to represent texture are wavelet-based features, Tamura features, and Local Binary Pattern (LBP) features.

Based on the fact that illumination has good robustness, the LBP texture feature extraction algorithm is used in this study [21]. The original LBP operator is defined in a square field centered on a pixel, generally using a 3×3 -neighborhood, with the pixel value of the point as the threshold, the grayscale values of the 8 adjacent pixels are compared with the pixel value in the center of the neighborhood, and the positions with pixel values greater than the center pixel value are marked with 1, and the ones that are less than are marked with 0. After a simple operation, the corresponding positions in the neighborhood can sequentially generate an 8-bit binary number, and then these 8 binary numbers are By arranging these 8 binary numbers in order, a binary number is formed, which is used to represent the LBP value of the center pixel, and there are 2^8 possibilities, i.e., 256 kinds of LBP values. The LBP value of the center pixel reflects the texture information of the area around the pixel. The formula for calculating LBP is shown in (11) (12):

$$LBP(x_c, y_c) = \sum_{p=0}^{p-1} 2^p s(i_p - i_c) \tag{11}$$

$$s(x) = \begin{cases} 1 & x \geq 0 \\ 0 & else \end{cases} \tag{12}$$

Where (x_c, y_c) is the coordinates of the center pixel, p is the prd pixel of the neighborhood, i_p is the gray value of the neighboring pixel, i_c is the gray value of the center pixel, and $s(x)$ is the sign function.

The improved circular LBP algorithm is selected in the texture feature extraction stage of this paper, i.e., the 3×3 -neighborhood is extended to an arbitrary neighborhood and the square neighborhood is replaced by a circular neighborhood, the improved LBP operator allows any number of pixel points in a circular neighborhood of radius R. A series of initially-defined LBP values are obtained by continuously rotating the circular neighborhood, and the minimum value is taken as the LBP value of the neighborhood. Compared with the original LBP algorithm, it is able to achieve the requirements of gray scale and rotation invariance. For a given center point (x_c, y_c) with neighborhood pixel positions (x_p, y_p), $p \in P$, its sampling point (x_p, y_p) is calculated using the following equation:

$$x_p = x_c + R\cos\left(\frac{2\pi p}{P}\right) \tag{13}$$

$$y_p = y_c - R\sin\left(\frac{2\pi p}{P}\right) \tag{14}$$

Where, R is the sampling radius, p is the prd sampling point and P is the number of samples.

The obtained LBP features are connected in a network with two convolutional layers, two activation layers, two pooling layers and one fully connected layer. The convolutional layers $kernel\_size = (3,3)$ and $filters = 32$, the activation function of the activation layer is "ReLu", the pooling layer is MaxPooling, and the number of neurons in the fully connected layer is 128. The final 128-dimensional vector is used as the LBP feature of the image and is denoted as x_2.

3.3. *Texture Feature Extraction*

Texture features can reflect the thickness, size, direction, roughness and smoothness of the oil painting strokes. The statistical features obtained by calculating the region with many pixel points are anti-interference and have rotational invariance. The extraction method of texture features chooses the gray scale covariance matrix, which can effectively describe the change information of the image at a certain distance and direction. Therefore, in this study, we choose to use the grayscale co-production matrix to calculate the texture features of Chinese oil paintings.

The grayscale covariance matrix is used to describe the relationship between two pixels of a given direction and distance in a target region. The grayscale co-production matrix is often used to reflect the grayscale variation of neighboring pixels in the target region of an image. In processing grayscale images, using the grayscale covariance matrix method, the extracted oil painting image is first grayscaled to construct a local grayscale covariance matrix of the diseased oil painting, and the eigenvalues such as energy, entropy, contrast, and correlation are calculated [22].

Energy - Energy is the sum of squares of the values of the elements of the grayscale symbiosis matrix, reflecting the uniformity of the image grayscale distribution and texture coarseness. If all the values of the co-production matrix are equal, the ASM value is small. Conversely, if some of the values are large and others are small, the ASM value is large:

$$ASM = \sum_{i=1}^{k}\sum_{j=1}^{k}(G(i,j)2) \tag{15}$$

Entropy - Entropy is a measure of the amount of information that an image has, texture information also belongs to the information of the image, it is a measure of randomness, entropy is maximum when all the elements in the covariance matrix have maximum randomness, all the values in the spatial covariance matrix are in phase, and the elements in the covariance matrix are dispersed and distributed:

$$ENT = -\sum_{i=1}^{k}\sum_{j=1}^{k}G(i,j)\log G(i,j) \tag{16}$$

Contrast - reflects the clarity of the image and the degree of depth of the texture grooves. The deeper the texture furrows, the greater the contrast and the clearer the visual effect. On the contrary, the contrast is small, the grooves are shallow and the effect is blurred:

$$CON = \sum_{n=0}^{k-1} n2\left(\sum_{|i-j|=n} G(i,j)\right) \tag{17}$$

Correlation - defines the similarity of the elements of the matrix in terms of rows or columns, reflecting the correlation between the gray values in some areas of the graph; a larger correlation indicates that the values of the elements in the matrix do not differ much, while a smaller correlation indicates a large difference:

$$COR = \frac{\sum\sum(i-\bar{x})(j-\bar{y})G(i,j)}{\sigma x \sigma y} \tag{18}$$

4. Deep learning-based method for recognizing cultural identity of Chinese oil painting art

4.1. *Regularized Extreme Learning Machine*

The mathematical model of the extreme learning machine is equation (19):

$$f_L(x) = \sum_{i=1}^{L}\beta_i G\left(a_i, b_i, x\right) \tag{19}$$

where L is the number of implied layer nodes. β_i is the weight coefficient of the i rd implicit layer node for the output node, where $\beta_i \in R$. $G\left(a_i, b_i, x\right)$ is the output function of the i th implicit layer node. a_i, b_i are the input weights and node bias of the i th implicit layer node, respectively, where $a_i \in R^n$, $b_i \in R$. $G\left(a_i, b_i, x\right)$ The output function can be expressed as Eq. (20):

$$G\left(a_i, b_i, x\right) = g\left(a_i \cdot x + b_i\right) \tag{20}$$

where $g(\cdot)$ is the activation function.

If there is N set of training set data $\{(x_l, y_l)\}_{l=1}^{N}$, x_l, y_l are input variables and output variables, where, $x_l \in R^n$, $y_l \in R^m$, then Eq. (21):

$$y_l = \sum_{i=1}^{L} \beta_i G(a_i, b_i, x_l), l = 1, 2, \cdots, N \tag{21}$$

The matrix form of Eq. (21) is Eq. (22):

$$H\beta = Y \tag{22}$$

The formula is as in equation (23):

$$\begin{gathered} H = \begin{bmatrix} G(a_1, b_1, x_1) & \cdots & G(a_L, b_L, x_1) \\ \vdots & \vdots & \vdots \\ G(a_1, b_1, x_N) & \cdots & G(a_L, b_L, x_N) \end{bmatrix} = \begin{bmatrix} h(x_1) \\ \vdots \\ h(x_N) \end{bmatrix} \\ \beta = \begin{bmatrix} \beta_1 \\ \vdots \\ \beta_L \end{bmatrix}_{L\times_m}, Y = \begin{bmatrix} y_1 \\ \vdots \\ y_N \end{bmatrix}_{N\times m} \end{gathered} \tag{23}$$

Since a_i, b_i are randomly generated and only β is obtained by $\{(x_l, y_l)\}_{l=1}^{N}$ computation, in order to improve the accuracy of the ELM, the ELM introduces a regularization factor λ, at which point solving β is transformed into the following optimization problem as Eq. (24):

$$\begin{gathered} \min_{\beta} : V_{ELM} = \frac{1}{2}\|\beta\|^2 + \frac{\lambda}{2}\sum_{l=1}^{N}\|\varepsilon_l\|^2 \\ s.t.: h(x_l)\beta = y_l - \varepsilon_l, l = 1, 2, \cdots, N \end{gathered} \tag{24}$$

where ε_l is the training bias, which mainly serves to avoid the overfitting problem. The optimization solution problem of Eq. (24) can be converted into the following dual optimization problem as Eq. (25):

$$V_{ELM} = \frac{1}{2}\|\beta\|^2 + \frac{\lambda}{2}\sum_{l=1}^{N}\|\varepsilon_l\|^2 - \sum_{l=1}^{N}\sum_{j=1}^{m} a_{l,j}\left(h(x_l)\beta_j - y_{l,j} + \varepsilon_{l,j}\right) \tag{25}$$

The optimal solution for β is calculated from Eq. (25) as Eq. (26):

$$\beta = H^T\left(\frac{I}{\lambda} + HH^T\right)^{-1} Y \tag{26}$$

From Eq. (26), β in RELM is mainly determined by matrix H, matrix Y and regularization factor λ in Eq. (23), where the dimension of H is related to the number of nodes of the implicit layer L and the number of training samples N, and Y is the output of the training samples, and the performance of the RELM is affected by the choice of the parameters of the number of nodes of the implicit layer L and the regularization factor λ, since N and Y have been determined.

In case of binary classification problem, the decision model of RELM is equation (27):

$$f(x) = sign\left(h(x)H^T\left(\frac{I}{\lambda} + HH^T\right)^{-1} Y\right) \tag{27}$$

In case of a multi-categorization problem, the decision model of RELM is equation (28):

$$label(x) = \underset{i\in(1,2,\cdots,m)}{\arg\max} f_i(x) \tag{28}$$

where $f_i(x)$ is the value of the first output node and $f(x) = [f_1(x), f_2(x), \cdots, f_m(x)]^T$.

4.2. RELM oil painting recognition method based on color features and texture features

For the oil painting image samples, the oil painting color features and texture features are extracted, and the feature vector $feature(i,j)$ of the oil painting image is equation (29):

$$feature(i,j)=\{Lr,Le,Ld,Lj,\mu,\sigma,\xi\} \tag{29}$$

The oil painting recognition process of KELM based on color features and texture features can be specifically described as follows:
1) Read the oil painting image sample data.
2) Extract oil painting image texture features and color features $feature(i,j)$.
3) Coding the category of oil painting.
4) Divide the feature vector $feature(i,j)$ of the oil painting image into training samples and test samples, take the feature vector $feature(i,j)$ of the oil painting image of the training samples as the input of RELM, and the categories of the oil paintings of the training samples as the output of RELM, and establish the RELM model.
5) For the test samples of oil painting images, the RELM oil painting recognition model is applied to recognize oil paintings.

The flowchart of the algorithm in this paper is shown in Fig. 1.

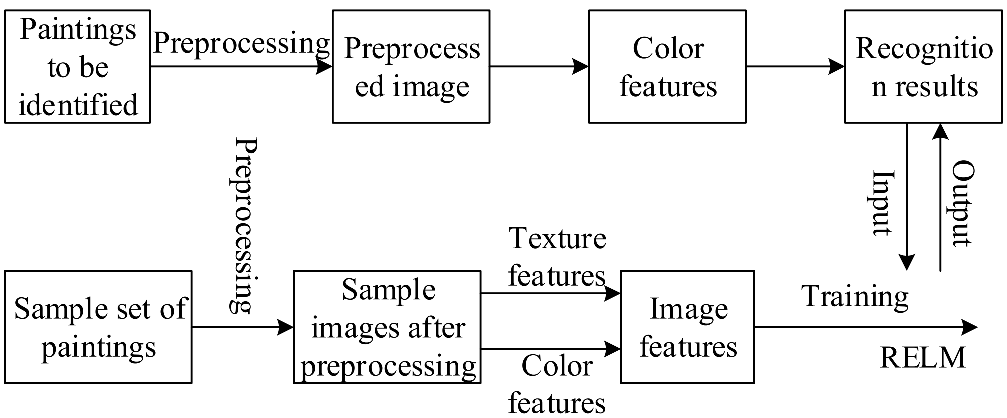

Fig. 1. The Oil painting identification flowchart based on RELM

5. Quantitative Research on the Cultural Identity Characteristics of Chinese Oil Painting Art

In this paper, Jin Shangyi's Cityscape series is selected as the training and testing samples to test the effectiveness of this paper's method in recognizing the cultural identity features of oil painting art. This series of oil paintings vividly depicts the changing urban landscape of China and portrays different cityscapes across China. The test set contains a total of 20 works, of which 15 are used as the training set and 5 as the test set.

5.1. Experiment and result analysis of oil painting feature set

Observation of a large number of oil paintings reveals that the oil painting subjects depicted in oil paintings can generally be summarized as: houses, bodies of water, vegetation, bare ground, roads. On the basis of describing the spectral and textural features, based on the method of this paper, we analyze the characteristics of various types of oil painting subjects, with a view to finding the features that can make a greater degree of differentiation between oil painting subjects, and constructing an attribute set that can effectively characterize the separateness between oil painting subjects.

5.1.1. Experimental analysis of spectral characteristics of oil painting subjects. Compared with RGB, HSV is better able to represent the connection and difference between perceived colors and keep simplicity in the computation process.HSV color space is more intuitive than RGB color space and is often used in color characterization. Therefore, in this paper, oil painting RGB color features are converted to HSV color space.

Under the HSV color quantization space, various types of oil painting subjects belong to different color quantization intervals. In order to find the distribution of road color information in HSV color quantization space, we mark the road hyperpixels for counting, manually extracted more than 10,000 road hyperpixels, and selected the corresponding quantization value with the largest number of pixels in the hyperpixels as the quantization value of the hyperpixels and analyzed them for color categorization.

The distribution of road superpixels in the HSV color quantization space is shown in Fig. 2. Among the counted road superpixels, close to 95% of the manually labeled road superpixels are distributed in the seven gray spaces of (8), and the roads account for less than 5% of the quantized color spaces (9-14). This also indicates that in the HSV color quantization space, the quantized grey scale space is able to include the color information of the roads in the oil painting image, which means that the roads are mostly in the non-color region.

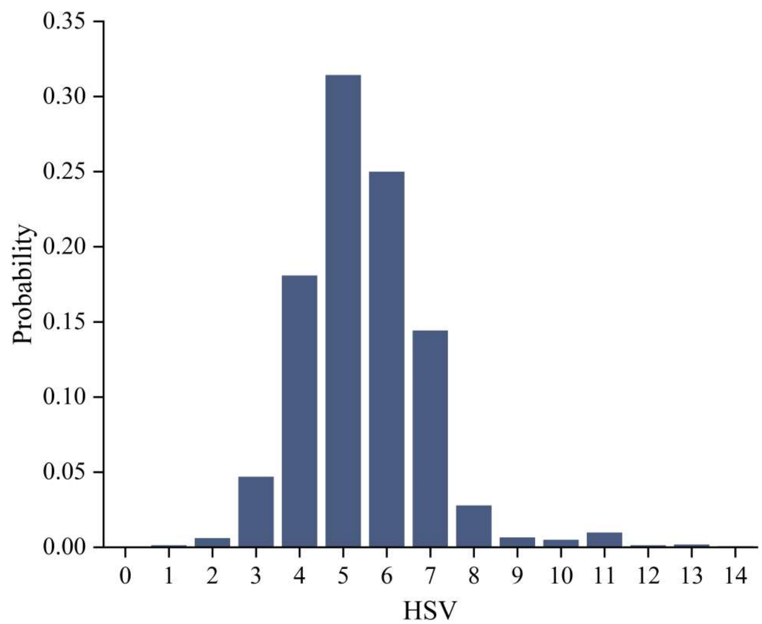

Fig. 2. The distribution of road superpixels in the quantitative space of the HSV color

In order to further analyze the distribution of various types of oil painting subjects in oil painting images under the color quantization space, after the oil painting subjects in oil painting images are classified into five categories: roads, houses, vegetation, bare ground and waters, the distribution statistics under the HSV color quantization space are carried out for various types of oil painting subjects, and the statistics of all types of oil painting subjects have more than 5000 superpixels, and the distribution of various types of oil painting subjects under the HSV color quantization space is shown in Figure 3. The distribution of each type of oil painting subject under HSV color quantization space is shown in Fig. 3, and Figs. (a)~(e) represent the distribution of superpixel color quantization of road, house, vegetation, bare ground and water, respectively.

Under the HSV color quantization space, most of the houses and roads are distributed in the grey scale space as well, except that some houses with bright color information can be eliminated. At the same time, some waters may fall into the grayscale space due to their dark color. Bare ground and vegetation hyperpixels are mostly able to be distributed in the quantized colored region due to their unique and small variation in color information.

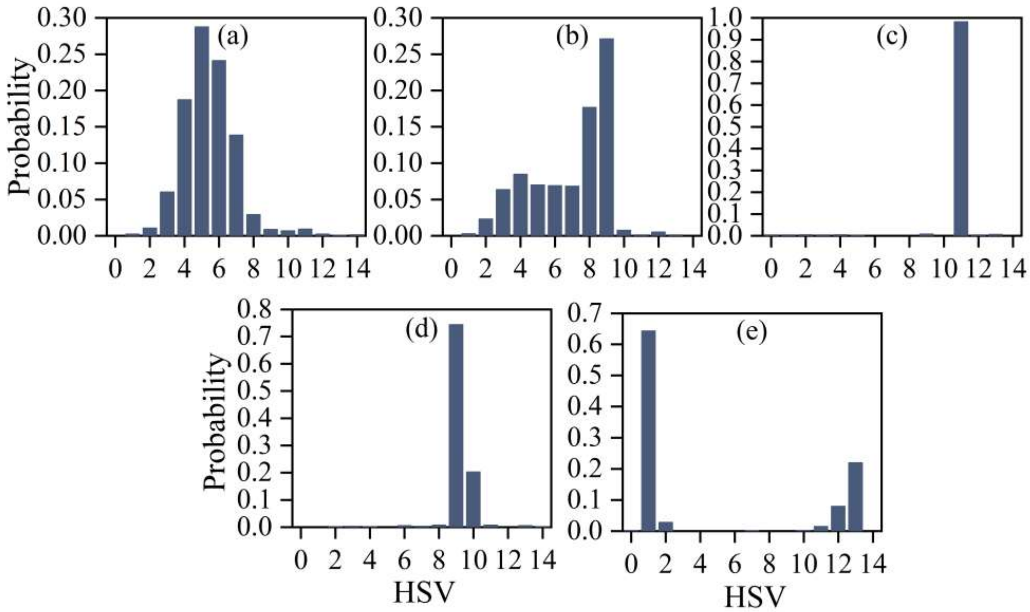

Fig. 3. The distribution of various objects in the quantitative space of HSV

The distribution of the five types of oil painting subjects in the HSV color quantization space illustrates that the single feature descriptive power of the color quantization space is still insufficient in distinguishing some of the oil painting subjects, which is reflected by the fact that most of the houses can not be effectively distinguished from the roads. Therefore, only relying on the HSV color quantization space to discriminate is not enough to extract feature information, and it is also necessary to characterize the road hyperpixels with feature patterns other than color features to enhance the separability between different oil painting subjects.

5.1.2. Experimental analysis of oil painting texture characteristics. In the oil painting image, all kinds of oil painting subjects, including roads, can be more clearly characterized in the image, and the surface details of the oil painting subjects are more fully displayed. Due to the similarity of surface spectral and textural characteristics of homogeneous areas, homogeneous oil painting subjects including roads and waters can be characterized as smooth areas in a darker form under the total variance of the neighborhood. The non-road areas with large variations in local spectral and textural information can be characterized as non-homogeneous areas by highlighting them under the neighborhood total variation feature.

In order to be able to characterize the neighborhood total variance feature based on hyperpixels, we select the mean and variance within the hyperpixel region for comparative analysis, and the results are shown in Fig. 4. Even under the Otsu threshold method segmentation, most of the regions of vegetation and house hyperpixels still exhibit irregularities in gray texture, resulting in both vegetation and houses being larger than roads in terms of the mean value of the total neighborhood variance. From the figure, it can be seen that the neighborhood total variance regional mean feature is effective in describing the roads, thus being able to alleviate the lack of relying on color information for characterization.

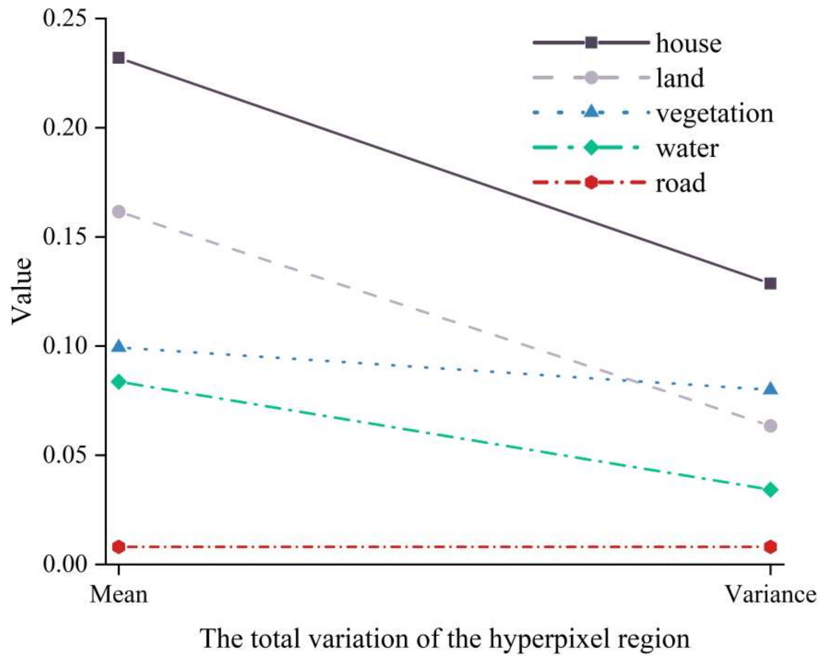

Fig. 4. Analysis of mean and variance

LBP texture characterization of roads is performed for effective feature extraction from the texture structure aiming to exclude the influence of factors such as illumination. Considering the number of feature dimensions as well as the characterization capability, a specific 9-dimensional uniform rotation invariant LBP descriptor is used for the texture characterization of the oil painting subject. Fig. 5 shows the distribution of the object super-pixel rotation invariant LBP descriptions, and Figs. (a) to (e) represent the feature space distribution of the rotation invariant uniform pattern LBPs for roads, houses, vegetation, bare ground, and waters, respectively.

As can be seen from Fig. 5, the difference in texture information of the oil painting subject is getting smaller and smaller due to the decrease in the dimension of the rotation invariant LBP, and the difference in the uniform rotation invariant LBP features of the road, house, vegetation, and water domain is smaller. However, it can be seen that the difference between the uniform rotation invariant LBP features of the water area and the other oil painting subjects is particularly obvious, i.e., the water area has a strong separability under this feature, which compensates for the interference caused by the fact that the water area is partially too dark under the spectral feature, which causes it to fall into the gray scale space.

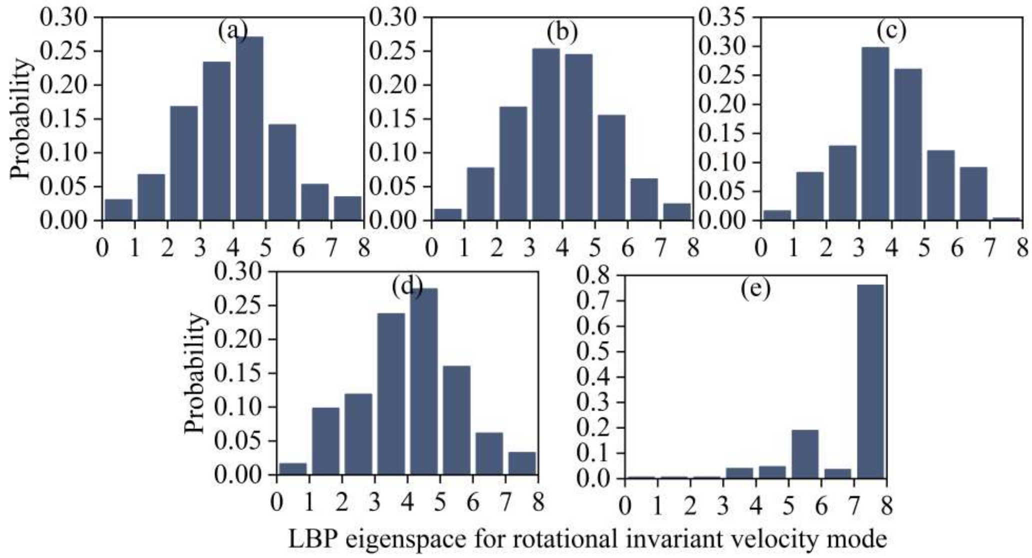

Fig. 5. The object super pixel rotation invariant LBP description distribution

Due to the deficiency in texture differentiation of oil painting subjects under uniform rotation invariant LBP features. In order to be able to provide a more powerful description of the texture features, the texture features are extracted from the hyperpixels by introducing a grayscale covariance matrix. Statistical calculations of the four texture features, energy, entropy, homogeneity and contrast, were performed in the oil painting image with the center of each superpixel region as the window center point at θ=(0°, 45°, 90°, 135°), respectively.

The experimental results show that, except for the bare ground and the road, the body of the oil painting has a high differentiation in entropy and contrast, then the bare ground and the road can be well extracted from the body of the oil painting, so we choose entropy and contrast as the parameter features of the grayscale covariance matrix. Considering also the previous distinguishability of bare ground and road in color features, it is therefore theoretically possible to extract feature information in oil painting images with complex separability.

5.2. Quantitative study of artistic and cultural identity

Using the features obtained by screening based on mathematical statistics and based on the imaging laws of deep forgery techniques, four groups of images are detected: real oil painting images and deep forgery images, identity replacement deep forgery images and identity preservation deep forgery images, real images and identity replacement deep forgery images, and real images and identity preservation deep forgery images.

5.2.1. Experimental results and analysis of selected features based on mathematical statistics. Using five models, XGBoost, logistic regression classifier, linear support vector machine, multilayer perceptron, and RELM, the test accuracy is shown in Table 1 for three groups of features: all features, filtered features (containing texture features, color components based on color moments, and color components based on texture features), and texture features, and the test accuracies are shown in Table 1, and the bolded values are the highest detection accuracies for each group.

Among the five types of algorithms, MLP and LP are less effective, XGBoost and LSVM are more effective, and RELM is unstable and affected by the type of classification, with the accuracy spanning from 53% to 86%, and the variability of different algorithmic models is large.

In group 1, screening features and texture features improve the accuracy over all features on XGBoost by 2.44% and 1.5%, respectively. Texture features improved the accuracy over all features on LSVM and MLP by 0.36% and 0.97%, respectively. And all features have the best detection on RELM with 86.69%, but the accuracy of all other feature groups is around 55%. In group 3, RELM has the highest detection accuracy among the three groups of features, followed by XGBoost and LSVM, and LR is the lowest. The accuracy of screening features on RELM is 1.71% better than all features. The accuracy of screening features on LSVM and MLP is improved by 0.50% and 1.71% over all features, respectively. It is also found that the accuracies of color components based on color moments are lower than the 99% PCA results for all features except for the RELM algorithm, which is almost 10% lower than the accuracies of all features.

Table 1. The precision of the classification algorithm based on quantitative data

Group	Model	All features	Screening feature	Texture characteristics
1	XGBoost	68.55%	70.99%	70.05%
	LR	64.97%	62.22%	65.33%
	LSVM	73.23%	71.90%	73.59%
	MLP	65.03%	61.86%	66.00%
	RELM	86.69%	56.01%	54.26%
2	XGBoost	61.36%	59.07%	54.39%
	LR	60.43%	59.40%	54.40%
	LSVM	62.27%	60.31%	58.29%
	MLP	58.62%	58.41%	52.13%
	RELM	64.46%	67.19%	53.07%
3	XGBoost	72.84%	71.63%	72.68%
	LR	65.62%	65.44%	62.82%
	LSVM	75.15%	75.65%	72.52%
	MLP	65.17%	66.88%	55.97%
	RELM	86.82%	89.51%	86.54%
4	XGBoost	68.61%	60.22%	
	LR	66.14%	56.00%	
	LSVM	74.71%	56.59%	
	MLP	62.47%	54.39%	
	RELM	59.63%	55.62%	

5.2.2. Experimental results and analysis of selected features of the imaging law of the depth forgery technique. Five models, XGBoost, logistic regression classifier, linear support vector machine, multilayer perceptron and RELM, are utilized to test the screening features on the self-constructed dataset and ForgeryNet dataset, in order to validate the universality of the features screened based on the imaging laws of the deep-fake technique.

The ForgeryNet data is divided into four sets of experiments:(1) Real images and deep-fake images. (2) Identity replacement deep-fake image and identity preservation deep-fake image. (3) Real Image and Identity Replacement Deep Fake Image. (4) Real image and identity preserved deepfake image.

Each set of experiments contained 3 sets of features:(1) Strongly correlated features. (2) Moderately correlated features. (3) Weak correlation features. The comparison of the four groups of detection results is shown in Fig. 6.

The results of the first set of experiments are shown in Fig. 6(a).The detection accuracy of the XGBoost and MLP algorithms is inversely proportional to the correlation.The LR, LSVM & RELM algorithms have the lowest detection accuracy when using the medium correlation features and the highest detection accuracy when using the low correlation features.

The results of the second set of experiments are shown in Fig. 6(b), the detection accuracy of XGBoost algorithm is directly proportional to the correlation. The detection accuracy of LR and LSVM algorithms is inversely proportional to the correlation. The MLP algorithm has the lowest detection accuracy when using low-correlation features, and has comparable detection accuracies when using high and medium-correlation features. The RELM algorithm has comparable detection accuracies when using the three sets of features.

The results of the third set of experiments are shown in Fig. 6(c), the detection accuracy of XGBoost, LR and LSVM algorithms is inversely proportional to the correlation. The MLP and RELM algorithms have the highest detection accuracy when using low correlation features.

The fourth set of experimental results Figure 6(d), the detection accuracy of XGBoost, LR & LSVM algorithms is inversely proportional to the correlation. And the detection accuracy of the five algorithms is much higher when using low correlation features than when using high and medium correlation features.

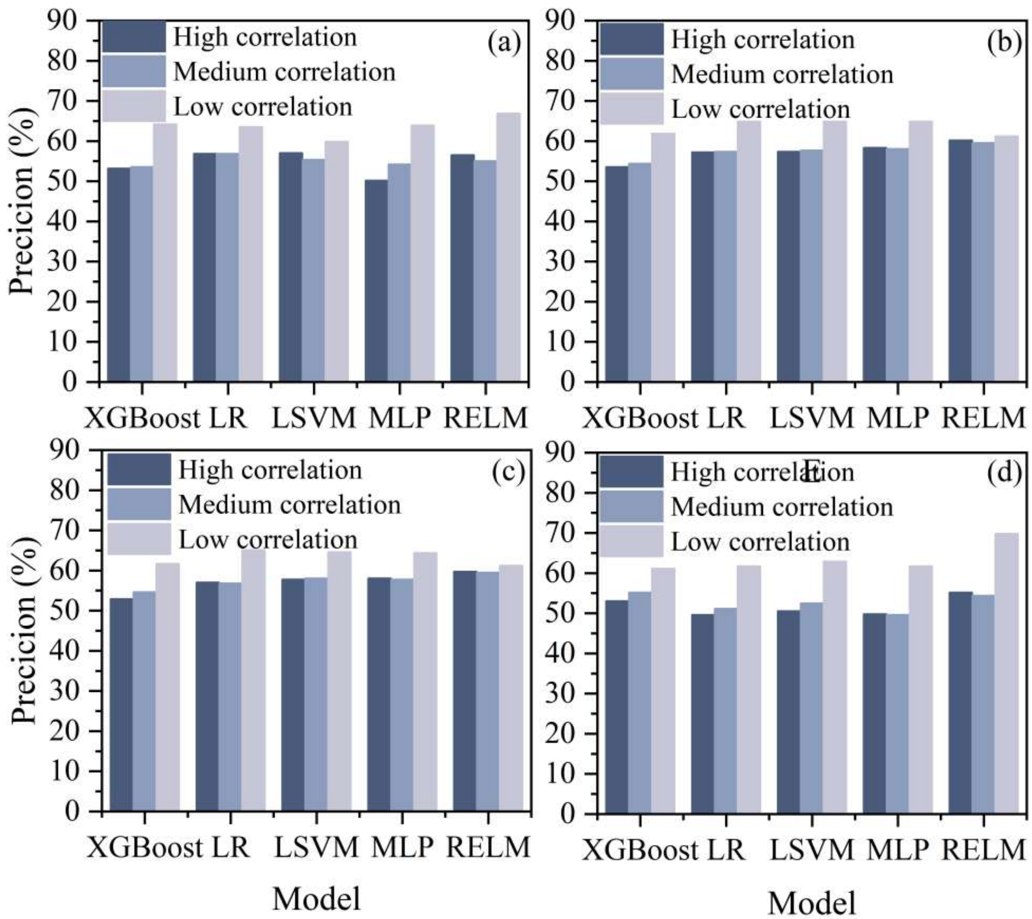

Fig. 6. Comparison of the results of the four groups

5.2.3. Comparison experiments and results with convolutional neural network applications. In order to test the feasibility of oil painting feature recognition based on quantized texture and color features, the experiments were conducted by selecting the current mainstream convolutional neural networks for deep forgery image detection to compare the detection accuracy. For the ForgeryNet image dataset, the convolutional neural networks used are, in descending order of the number of total parameters, ResNet50V2, XceptionNet, EfficientNetV2S, EfficientNetB4, DenseNet121, and MobileNetV2. The results of the detection of oil painting images based on different convolutional neural networks are shown in Fig. 7.

The six networks have different detection accuracies for the same group of images, and each network has different detection accuracies for different groups of images.EfficientNetB4 has the lowest detection accuracy, which is only around 55%.ResNet50V2, DenseNet121 & MobileNetV2 have better detection results, which are all higher than 70%. Overall, the results of groups 3 and 4 are better than those of groups 1 and 2.

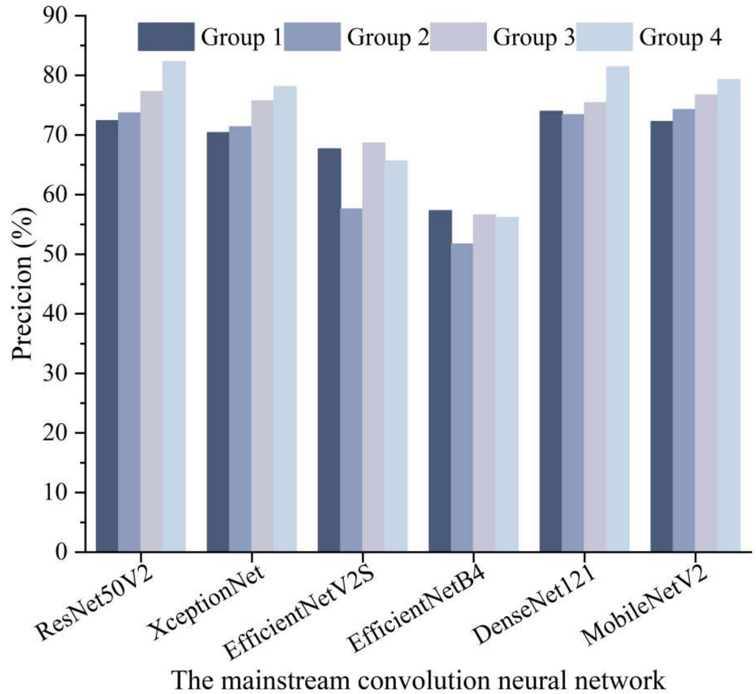

Fig. 7. Different convolution neural network detection results

Combining the quantized data detection results in Table 1 and Figure 7, it is found that:
1) The detection accuracy of the quantized data obtained from screening based on mathematical statistics using RELM and XGBoost algorithms is higher than the detection accuracy using convolutional neural networks. The detection accuracy of the quantized data screened based on the imaging law of deep pseudo technology is not as good as that of the convolutional neural network.
2) Regardless of the method of detection, the detection accuracy of group 2 is poor, and the detection accuracy of groups 3 and 4 is higher. Therefore, in the case of comparable or even higher accuracy, quantized data-based detection is more efficient.

6. Conclusion

In this paper, global color histogram and LBP are used to identify the color and texture features of Chinese oil paintings, and the Extreme Learning Machine (ELM) is regularized to use the improved RELM model for the recognition of artistic and cultural identity features of Chinese oil paintings. The oil painting "Cityscape" is used as the training and testing dataset. The experiments show that the neighborhood total variation sub-area mean feature is effective in describing the oil painting objects, which alleviates the deficiency of relying on color information characterization to a certain extent. The method in this paper can effectively separate and extract the texture information of the oil painting subject, and the oil painting color and texture detection accuracy achieves optimal performance in most of the experimental groups, and the RELM algorithm has the highest detection accuracy at low correlation features. Therefore, it shows that the oil painting feature recognition method provided in this paper can accurately recognize the identity features of different oil painting subjects, which is convenient for further quantitative research.

References

[1] Shrestha, A., & Mahmood, A. (2019). Review of deep learning algorithms and architectures. IEEE access, 7, 53040-53065.

[2] Pouyanfar, S., Sadiq, S., Yan, Y., Tian, H., Tao, Y., Reyes, M. P., ... & Iyengar, S. S. (2018). A survey on deep learning: Algorithms, techniques, and applications. ACM computing surveys (CSUR), 51(5), 1-36.

[3] Lauriola, I., Lavelli, A., & Aiolli, F. (2022). An introduction to deep learning in natural language processing: Models, techniques, and tools. Neurocomputing, 470, 443-456.

[4] Wang, P., Fan, E., & Wang, P. (2021). Comparative analysis of image classification algorithms based on traditional machine learning and deep learning. Pattern recognition letters, 141, 61-67.

[5] Feng, J. (2023). The Spirit of Freehand Brushwork in Chinese Oil Painting. Pacific International Journal, 6(1), 56-60.

[6] Dong, Z. (2021, December). Discussion on the Value Experience and Language Connotation of Modern China's Expressive Oil Painting. In The 5th International Conference on Art Studies: Research, Experience, Education (ICASSEE 2021) (Vol. 1, pp. 224-228). Amsterdam University Press.

[7] He, Z. (2023). Exploration on Localization of China's Oil Paintings-Research on Image Oil Painting. Art and Performance Letters, 4(8), 40-43.

[8] Ma, X. (2024). The Influence of Chinese Folk Art on Modern Oil Painting. Art and Performance Letters, 5(1), 112-119.

[9] Zixuan, G. (2022). A Study of the Ethnicity of Chinese Oil Painting. Frontiers in Art Research, 4(15).

[10] Hongxian, L., Tahir, A., Bakar, S. A. S. A., Omar, A., & Baharom, M. K. (2024). Applying the Elements of Traditional Chinese Painting in Chinese Oil Painting Creation. Kurdish Studies, 12(2), 3850-3859.

[11] Wang, R. (2019, January). Research on Chinese Elements in Modern Oil Painting Creation. In 2018 International Workshop on Education Reform and Social Sciences (ERSS 2018) (pp. 409-412). Atlantis Press.

[12] An, Z., & Nie, D. (2023). Impact Of Chinese Cultural Elements On Spiritual Expression In Oil Painting Imagery Landscape: An Exploratory Study In Arts Education. Arts Educa, 37.

[13] Xing, C., & Pinyonatthagarn, D. (2023). The Development And Exploration Of Realist Oil Painting In Contemporary China And Russia. Journal of Namibian Studies: History Politics Culture, 33, 3574-3596.

[14] Li, L. (2023). Multiple expression forms and their aesthetic trend of modern Chinese image oil painting. Frontiers in Art Research, 5(18).

[15] Sun, S., & Wang, K. (2023). An Introduction to the Influence of Neo-expressionism on Contemporary Chinese Oil Painting. Journal of Humanities, Arts and Social Science, 7(8).

[16] Fan, L. (2021). THE LATEST TRENDS IN THE MODERN OIL LANDSCAPE PAINTING OF CHINA. European Journal of Arts, (4), 143-147

[17] Yang, G. (2021). The imagery and abstraction trend of Chinese contemporary oil painting. Linguistics and Culture Review, 5(S2), 454-471

[18] Cui, F. B. (2023). A Probe into the Modernity of Chinese Oil Painting. International Journal of Advanced Culture Technology, 11(1), 198-203.

[19] Yan Qing Wang,Lu Lu Zhuang & Chao Xia Shi. (2014). Construction Research on Multi-Threshold Segmentation Based on Improved Otsu Threshold Method. Advanced Materials Research(1046-1046),425-428.

[20] Pooja Ch. & K Jaisharma. (2022). Novel Framework for the Improvement of Object Detection Accuracy of Smart Surveillance Camera Visuals Using Modified Convolutional Neural Network Technique Compared with Global Color Histogram. Electrochemical Society Transactions(1).

[21] Nitin Arora,Ishan Budhiraja,Deepak Garg,Sahil Garg,Bong Jun Choi & M. Shamim Hossain. (2025). Revolutionizing facial image retrieval: Multi-block and mean based local binary patterns with sign and magnitude analysis. Alexandria Engineering Journal601-608.

[22] Chao Zhang,Yang Yang,Yaoyao Zhang,Qingchao Sun,Kai Li & Chenchun Shi. (2025). Quantitative evaluation of the connection status of an aeroengine rotor assembly interface with vibration energy flow and a gray level co-occurrence matrix. Mechanical Systems and Signal Processing112300-112300.